AD-A188 185 AUTOCORRELATION OF CONTROL POINTS ON 11-BAND MULTISPECTRAL IMAGERY(U) ARMY ENGINEER TOPOGRAPHIC LABS FORT BELVOIR VA R S RAND AUG 87 ETL-0473 1/1

UNCLASSIFIED F/G 12/9 NL

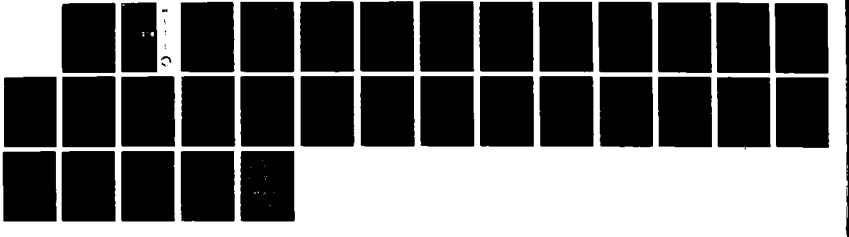

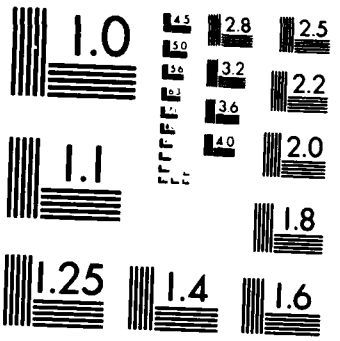

MICROCOPY RESOLUTION TEST CHART
NATIONAL BUREAU OF STANDARDS-1963-A

ETL-0473

Autocorrelation of Control Points on 11-Band Multispectral Imagery

Robert S. Rand

August 1987

Prepared for
U.S. ARMY CORPS OF ENGINEERS
ENGINEER TOPOGRAPHIC LABORATORIES
FORT BELVOIR, VIRGINIA 22060-5546

Destroy this report when no longer needed.
Do not return it to the originator.

The findings in this report are not to be construed as an official Department of the Army position unless so designated by other authorized documents.

The citation in this report of trade names of commercially available products does not constitute official endorsement or approval of the use of such products.

UNCLASSIFIED

SECURITY CLASSIFICATION OF THIS PAGE

REPORT DOCUMENTATION PAGE

Form Approved OMB No. 0704-0188

AD-A188 185

1a. REPORT SECURITY CLASSIFICATION: UNCLASSIFIED	1b. RESTRICTIVE MARKINGS
2a. SECURITY CLASSIFICATION AUTHORITY	3. DISTRIBUTION / AVAILABILITY OF REPORT: Distribution limited to U.S. Government agencies only; Operational Use; August 198(Other requests for this document must be referred to Comman and Director, U.S. Army Engineer Topographic Laboratories, Fort Belvoir, VA 22060-5546
2b. DECLASSIFICATION / DOWNGRADING SCHEDULE	
4. PERFORMING ORGANIZATION REPORT NUMBER(S): ETL-0473	5. MONITORING ORGANIZATION REPORT NUMBER(S): ETL-0473
6a. NAME OF PERFORMING ORGANIZATION: U.S. Army Engineer Topographic Laboratories; 6b. OFFICE SYMBOL (If applicable)	7a. NAME OF MONITORING ORGANIZATION
6c. ADDRESS (City, State, and ZIP Code): Fort Belvoir, VA 22060-5546	7b. ADDRESS (City, State, and ZIP Code)
8a. NAME OF FUNDING / SPONSORING ORGANIZATION; 8b. OFFICE SYMBOL (If applicable)	9. PROCUREMENT INSTRUMENT IDENTIFICATION NUMBER
8c. ADDRESS (City, State, and ZIP Code)	10. SOURCE OF FUNDING NUMBERS

PROGRAM ELEMENT NO.	PROJECT NO.	TASK NO.	WORK UNIT ACCESSION NO.
63701B	3205	E	D60

11. TITLE (Include Security Classification)

Autocorrelation of Control Points on 11-Band Multispectral Imagery

12. PERSONAL AUTHOR(S)
Robert S. Rand

13a. TYPE OF REPORT	13b. TIME COVERED	14. DATE OF REPORT (Year, Month, Day)	15. PAGE COUNT
Technical Report	FROM _____ TO _____	August 1987	26

16. SUPPLEMENTARY NOTATION

17. COSATI CODES		
FIELD	GROUP	SUB-GROUP

18. SUBJECT TERMS (Continue on reverse if necessary and identify by block number)
Autocorrelation Measures, Image Registration, Multispectral Imagery, Feature Extraction, Image Segmentation Algorithms.

19. ABSTRACT (Continue on reverse if necessary and identify by block number)

The use of multispectral imagery with other types of imagery requires that the combined set be accurately registered. This study investigates correlation properties between bands of an 11-channel multispectral scanner for 37 control points in support of interband registration that can later be extended to dissimilar image registrration. The results sho a high degree of correlation between channels 1 through 7, but a lower and unpredictable correlation for other combinations. In addition to providing information about interband registration, the resu lts also have implications for multispectral segmentation algorithms.

20. DISTRIBUTION / AVAILABILITY OF ABSTRACT	21. ABSTRACT SECURITY CLASSIFICATION
☒ UNCLASSIFIED/UNLIMITED ☐ SAME AS RPT ☐ DTIC USERS	UNCLASSIFIED

22a. NAME OF RESPONSIBLE INDIVIDUAL	22b. TELEPHONE (Include Area Code)	22c. OFFICE SYMBOL
E. James Books	202-355-3039	CEETL-IM-T

DD Form 1473, JUN 86 — Previous editions are obsolete.

SECURITY CLASSIFICATION OF THIS PAGE
UNCLASSIFIED

PREFACE

This study was conducted under Program Element 63701B, Project Number 3205, Task E, Work Unit D60, "Multisensor Image Exploitation".

The study was performed in 1985 under the supervision of Mr. Dale Howell, Chief, Information Sciences Division; and Mr. Lawrence Gambino, Director, Computer Sciences Laboratory.

COL Alan L. Laubscher was Commander and Director, and Mr. Walter E. Boge was Technical Director of the Engineer Topographic Laboratories during the report preparation.

TABLE OF CONTENTS

INTRODUCTION 1

DESCRIPTION OF EXPERIMENT

Image Set 2
Control Point Information 3
Autocorrelation Procedure 4

RESULTS OF EXPERIMENT 5

DISCUSSION 8

CONCLUSIONS 10

APPENDIX A: Control Point Information

APPENDIX B: Table of Correlation Values

APPENDIX C: Graphs of Incremented Correlation Values

APPENDIX D: Clustering of Control Points

INTRODUCTION

The concept of using multiple image sources from different sensors to perform semi-automated feature extraction and generate cartographic products brings forth numerous issues. In addition to the large amounts of digital data that accumulate in multiple image sets, each sensor inherently generates its own geometric and spectral parameters. Obviously, one reason for supplementing conventional mapping photography with imagery from other sources such as radar or multispectral scanners is because of the additional information they provide. However, along with this increase of information comes the difficulty of coordinating one image set to another. Differences in scale, orientation, and perspective, as well as distortions particular to each sensor must be accomodated before images from different sensors can be overlayed on top of one another or registered to a map source.

Numerous methods have been developed that attempt to register one image type to another. Basically, these methods fall into two categories: pixel-based correlation and feature-based correlation. In pixel-based correlation, a correlation process is applied to the gray shade values of an image pair in an attempt to match corresponding points. Once a sufficient number of points have been matched, the image coordinates of these points can be used to construct, by the method of least squares, a registration model mapping one image to the other. As can be expected, the difficulties using this method occur in the matching process. Gray shade values of a feature on two dissimilar image bands are likely to be different even though the underlying structural patterns of these gray shades are similar. Simple correlation measures cannot take structure into account.

Feature-based correlation methods attempt to remedy the problems of pixel-based methods by removing the effect of gray shade variation and correlating on the structure of features. These methods are concerned with generating a binary image pair that depict feature patterns common to the parent dissimilar image pair, and subsequently correlating the binary images. Generally, this method appears more promising then pixel-based correlation. One study in particular, a "Study of Digital Matching of Dissimilar Images" performed for ETL obtained rather favorable results using feature-based correlation on optical/radar image pairs.[1,2]

The experiment discussed in this report studies the correlation problem associated with pixel-based methods using imagery collected by an experimental 11-band Bendix Modular Multispectral Scanner (MMS) aboard an aircraft platform. Measures of autocorrelation between one MMS band and another were extracted by computer for 37 control points, and the results were then graphed for comparison. The use of this MMS imagery containing relatively narrow spectral bandwidths

provides a means to test the effect of spectral factors on correlation independently of the geometric factors that also create problems for pixel-based methods. In order to provide an adequate reference for comparison, an analysis of 1:18400 aerial photography and an analysis of 1:50000 map data was made to construct brief sentences to describe each of the control points.

In addition to applying correlation methods to image registration problems, the possibility exists that measures of autocorrelation might be useful to develop image primitives for use in algorithms directed at semi-automatic feature extraction. Therefore, the behavior of correlation across image bands was noted for possible implications toward this application.

DESCRIPTION OF EXPERIMENT

IMAGE SET. The imagery used in the experiment contains 11 bands of multispectral data that was collected by a Bendix Modular Multispectral Scanner (MMS) aboard a CORVAIR 580 aircraft in July 1981. Each band of imagery contains 8-bit data of 3000 lines by 803 pixels. The pixel size for these images corresponds to approximately 5 meters by 5 meters on the ground at nadir; but this increases to 5 meters by 8 meters at the far edge of the image. The wavelengths associated with these 11 bands are as follows:

MMS Wavelengths (microns)

Band	Wavelength	Band	Wavelength
1	0.38 to 0.44	7	0.66 to 0.70
2	0.44 to 0.49	8	0.70 to 0.74
3	0.49 to 0.54	9	0.76 to 0.86
4	0.54 to 0.58	10	0.97 to 1.05
5	0.58 to 0.62	11	8.00 to 12.0
6	0.62 to 0.66		

Unfortunately, this aircraft-based MMS system does not have the geometric fidelity to generate map products. However, its advantage as an experimental sensor is that it provides better spectral and spatial resolution than any of the currently operational multispectral sensors, including LANDSAT's Thematic Mapper. The increase in spectral and spatial resolution provides an opportunity to explore the advantages of high-resolution multispectral systems, and the additional problems that surface in coordinating large-scale dissimilar data.

The imagery is actually part of a larger set of multisensor imagery that has been provided to the Defense Mapping Agency (DMA), and that also resides on ETL's CYBER system. Called the ISP Data Set, this larger set of imagery includes panchromatic, multispectral, and radar imagery, as well as a digital terrain matrix -- all over a common geographic area. The 37 control points used in this study are defined with respect to this data set. For further information, see the documentation on the ISP Data Set.[3]

The scene contains a fairly large area (5 km by 15 km) of Freiburg, Germany and its surrounding area. There is a fairly good sampling of both urban and rural features. The 37 control points are easily identifiable points, such as a road intersecting with another road, a road intersecting a railroad, and boundary lines. In some cases, tree canopies obscure the view of the underlying control point; however, some kind of boundary usually exists to make the identification possible.

CONTROL POINT INFORMATION. An analysis of aerial photography and associated map data was made manually to collect information about each of the 37 control points. This was done so that there would be a basis on which to interpret the experimental data. With this information available it is possible to study the correlation data and understand the data in terms of the ground features it is representing. If the correlation graphs of two points are similar, there ought to be some physical reason for the similarity; likewise, if they are dissimilar, there ought to be some reason. In addition, the robustness of the correlation measure can be tested. If a group of control points is known to be physically similar and yet their correlation graphs are different, then the measure is not very robust nor useful.

Source material for performing the photo and map analysis was obtained from the ISP Data Set. The photo analysis was done on the 1:18400 transparencies that were the source of the digitized optical imagery in the ISP Dataset. The map analysis was done on the 1:50000 scale map (dated 1978) provided with this data set. For more information on this material, see the data set documentaion.

The control point information was compiled into brief sentences describing the most significant attributes of each point and its immediate vicinity. These sentences were carefully constructed so as to contain a limited set of descriptive parameters. For example, roads are labeled as one of four types: highways, main roads, secondary roads, and tertiary roads. The widths of the roads decrease from highways to tertiary. Highways and main roads are hard surfaced roads;

whereas, secondary roads are lightly surfaced, and tertiary roads are unsurfaced. In addition, road intersections are described spatially as an "X", "Y", or "T" intersection. Also, because correlation windows have a finite size, the background surrounding the immediate vicinity is also described. A table listing these sentences along with an ISP Dataset reference number is found in Appendix A.

AUTOCORRELATION PROCEDURE. Two sets of autocorrelation measures were collected for each of the 37 control points. One set was obtained by correlating Band 1 of the imagery with Band 2 through Band 10, using a 9 by 9 correlation window; this procedure generated a set of 10 values. The other set was obtained in a similar manner using a 15 by 15 correlation window. The procedure was repeated for all 37 control points. Note that because the spectral response of Band 11 (a thermal infrared band) was significantly different from the other bands, Band 11 was not used in the experiment. Also, note that the correlation procedure could have been repeated for additional band combinations; Band 2 with Band 3, Band 2 with Band 4, etc. However, such combinations are numerous, and a decision was made to limit the combinations unless the results warranted otherwise.

A table of the correlation results was assembled, and is presented in Appendix B. By definition, a correlation value "R" can range from -1 to +1; where a value of +1 indicates two windows are statistically identical; a value of zero indicates no statistical relationship (the windows are uncorrelated); and a value of -1 indicates the windows are statistically flipped (as a positive image is related to its photographic negative).

Graphs of the correlation measures were made by plotting the correlation values using a DEC microcomputer. Because of the limitations of the plotting routine to handle only positive numbers, the actual R values listed in Appendix B were incremented by +1 in the graphs. Defined as $C = R + 1$, the range of these incremented correlation values would be 0 to +2. Therefore, an incremented correlation value of +2 corresponds to an R value of +1 (statistically identical); an incremented value of +1 corresponds to an R value of 0 (no correlation); etc. These graphs are presented in Appendix C.

RESULTS OF EXPERIMENT

As mentioned above, Appendix A contains a description of each of the control points in as succinct a form as possible. Key phrases are standardized so that it is possible to identify similar categories of features. For example, a glance at the descriptions of control points 2, 7, and 26 easily shows that 2 and 7 are similar, whereas, 7 and 26 are significantly different (this observation will later be used to show a rather disturbing behavior of the correlation measure across certain bands). For the purpose of pixel-based correlation, shape descriptors such as "X" intersection or "T" intersection are perhaps irrevelant; however, they were included in case this proved not to be so.

Appendix B provides a list of correlation values for each control point with band combinations B1 and B2, B1 and B3, ... B1 and B10. The most obvious trend in these values is that the correlation values are very high and stable for band combinations up to B1/B7 for most control points. Another trend is the quick drop in correlation at B1/B8, as well as the numerous negative correlation peaks at band combinations B1/B9 and B1/B10 for various control points.

Appendix C contains graphs for the 37 control points that can be used to identify additional trends of the autocorrelation data. Note that the trends mentioned above are easily confirmed by the corresponding graphs; namely, the general stability of correlation values for band combinations up to B1/B7, the drop in correlation values for B1/B8, as well as the drop to negative values for B1/B9 and B1/B10. The exceptions and extremes of this behavior are easily spotted (i.e. control points 6, 12, 15, 17, and 35). In addition, one can conclude that the graphs of correlation values for W=9 generally follow those for W=15. Because W=15 is computationally more intensive then W=9 and offers no significant improvement, further analysis of the data can be restricted to the set of W=9 values.

The significance of a high R value at some image point is that registration between bands at such a point should be highly reliable. The graphs indicate that registration between any of B1 through B7 should be possible for all the control points, except for Point 12. Note that although the correlation values are made with respect to B1, one may infer by simple deductive reasoning that any combination of two bands up through B7 (e.g. B3 and B5) should also generate values near R=1.

In the case of Control Point 12, correlation values between B1 and any of the other bands for W=9 are never greater than R = 0.54. However, because the autocorrelations were made with respect to B1, the difficulty may disappear if the correlations were made with respect to B2, B3, ... or B7. This is likely because the R values are fairly stable for B2 through B7. Note that the physical nature of this

point is different from any of the others, with possible exception of Control Point 9. Although the map data records this point as an intersection between a road and a canal, this fact is obscured in the photo by trees, and the point appears as the corner of a forest and field. Although one sample is not enough to judge, this may suggest that interband registration of points in areas of natural vegetation may be difficult, even in B1 thru B7.

Beyond B7, the R values for most control points become significantly lower, suggesting difficulty in registering B8, B9, and B10 with the other bands. This is particularly true of B8, where the R values tend to be close to zero. In many cases, the R values of B9 and B10 are close to -1 (i.e., points 4, 10, 29, and 33), and are probably indicative of reliable registration; however, the corresponding ground features are not always that different from other control points that have weakly negative correlation (compare points 33 and 34). Therefore, apriori knowledge of a ground feature may not be sufficient to determine that there will be a large enough negative correlation to confidently register the point. Note that other than those points that generate strong negative correlation, the correlation values for B9 and B10 were generally weak.

Further comparison of the correlation graphs in Appendix C with the table in Appendix A shows that it is difficult to make a correspondence between graph trends and the physical nature of certain control points. Note the disturbing behavior of R values for the following control points:

* Point 2 vrs. 7: Similar feature types, different graphs.
* Point 7 vrs. 26: Different feature types, similar graphs.
* Point 1 vrs. 24: Different feature types, similar graphs.
* Point 35 vrs. 36: Similar feature types, different graphs.

Generally, this behavior lies with B1/B8, B1/B9, and B1/B10 combinations, rather than with the lower band combinations.

In order to gain additional insight into the behavior of B1/B9 and B1/B10 correlation values for the various control points, the table in Appendix D was constructed under the guidance of the graph trends in Appendix C and using the data in Appendix B for W=9. This table segments the control points into clusters according to the degree of difficulty expected in registering either B1/B9 or B1/B10. There are four clusters, indicating four levels of difficulty: no difficulty, questionable difficulty, probable difficulty, and extreme difficulty. Except where noted, the clusters refer to the level of difficulty for both B1/B9 and B1/B10 combinations. In the case of exceptions, the applicable band combination is indicated in parenthesis. Note that the degree of difficulty for registering bands is related to the magnitude of the R value and not the sign. Therefore, it ought to be possible to reliably register band combinations with R values close to -1.

The table in Appendix D further indicates a disturbing behavior of the correlation results. Whereas control points 1, 2, 4, 7, and 15 contain almost identical features, these points break into two very different clusters. Points 1, 2, and 15 are in the extreme difficulty cluster; however, points 4 and 7 are in the no difficulty cluster. The structural difference ("X" or "T") does not seem to be a factor because although points 1 and 7 have this differing structrual characteristic and are in different clusters, points 4 and 15 also have this difference but are in the same cluster. Structural similarity as with points 7 and 15 does not seem to significantly strengthen correlation, since these two very similar points are still in two very different clusters. It may be argued that the "almost invisible canal" contained in Point 7 but not in Point 15 was the distinguishing difference; however, this factor did not help Point 2.

Arguments of the types given above could continue endlessly for the various other control point comparisons, but one thing is clear. Spectral-related factors contributing to the lack of R robustness are too complex to currently incorporate into a semi-automated registration process. In addition, this experiment has excluded the geometric factors that also affect the registration process between dissimilar images. The combination of spectral and geometric related problems on pixel-based correlation methods for dissimilar image registration are likely to prove more troublesome.

DISCUSSION

This study has been directed at examining spectral factors that might inhibit pixel-based correlation methods from achieving reliable registration results. In a generalized dissimilar image scenerio, of course, not only do spectral factors have the potential to become troublesome, but so also will geometric factors such as scale difference, orientation, and stretching affect the process. These other factors have been eliminated in this study by selecting an 11-band multispectral image with the same relative geometry from one band to the next. Note that if spectral effects on pixel-based correlation are neglible, geometric effects still need to be examined, whereas, if spectral effects have a significantly negative impact, this negative impact is enough reason to dismiss the method regardless of geometric factors.

The results show that so long as the domain of control points is restricted to the type used in this study the effects of spectral factors on pixel-based correlation are neglible for dissimilar imagery within the visible spectrum. This is because of the very high and stable correlation values attained on band combinations B1/B2 through B1/B7 for almost all control points. The spectral range of B1 through B7 is 0.38 to 0.70 microns, and the narrow bandwidth of this imagery effectively has generated 7 continuous slices through this range, providing representative samples of most dissimilar imagery in the visible range. Therefore, any difficulty in registering dissimilar imagery within the visible spectrum using pixel-based correlation methods is not due to spectral factors, but rather it is due to geometric factors such as scale difference, orientation, and stretching.

There was one major exception to the stable correlation trend for the B1/B2 through B1/B7 combinations; namely, for control point 12 correlation values were weak throughout. In this case, the underlying features of point 12 were significantly different, indicating that for naturally occurring intersections such as the corner of forest and field boundaries there may be correlation problems introduced by the spectral variation of natural vegetation in various visible bands.

The generally encouraging results for visible band combinations, however, do not follow for visible-to-infrared band combinations. Beyond the B1/B7 combinations, the results show that spectral factors impose a negative effect on correlation. For most control points, there was a sharp drop in correlation at B8 (0.70 to 0.74 microns) that continued further with B9 (0.76 to 0.86 microns) and B10 (0.97 to 1.05 microns). Although the band combinations tested only B1/B8, B1/B9, and B1/B10, other combinations of visible bands with infrared bands such as B2/B8, B3/B8, ... B6/B10 are likely to yield similar results because of the stable and high correlation values of the visible band combinations.

For some control points the correlation values for B1/B9 and B1/B10 approached R=-1, indicating that these points could be successfully matched across such broad spectral ranges. However, the conditions under which this occur are not stable enough to identify any reliable cause and effect relationship. The results show that whereas some points generate correlation values close to R=-1, other very similar points produce values close to R=0. No explanation based on the underlying physical characteristics of the control points could be offered for this behavior. Therefore, although spectral factors may not impede pixel-based correlation methods of registering visible to infrared images in some cases, such special cases were not reliably identified, and this method of approach cannot be recommended for visible-to-infrared image registration.

With regards to feature extraction, evidence supporting the use of autocorrelation as an image primitive was not found. However, some helpful hints regarding the use of the 10 MS bands of imagery for feature extraction can be inferred from the data. Since correlation values close to +1, by definition, indicate that the information provided by two sources are redundant, the robust correlations of B1 through B7 show that there is little information to be gained by using more then one of these bands for segmenting the features of these control points. On the other hand, the fluctuations in correlation for B8, B9, B10 show there is additional information in these bands that could aid segmentation algorithms. However, as mentioned above, these fluctuations were not stable enough to identify any cause and effect relationship.

CONCLUSIONS

(1) The effects of spectral factors on pixel-based correlation methods for registering dissimilar imagery are negligible within the visible spectrum, so long as the domain of control points is restricted to the types used in this study.

(2) There may be correlation problems introduced by the spectral variation of natural vegetation in various visible bands.

(3) Spectral factors impose a negative effect on pixel-based correlation methods for registering visible to infrared imagery.

(4) Because of the negative impact of spectral factors on pixel-based correlation, feature-based correlation ought to be considered as an an alternative to pixel-based methods for registering dissimilar images.

(5) Evidence to support the use of autocorrelation measures as image primitives for feature extraction was not found. However, this measure is useful to determine which bands of imagery contain redundant information, and which bands contain additional information that might be useful to improve the performance of multicomponent segmentation algorithms.

REFERENCES

(1) Barbara Lambird, David Lavine, George Stockman, Kenneth Hayes, and Laveen Kannal; "Study of Digital Matching of Dissimilar Images", prepared for U.S. Army Engineer Topographic Laboratories, Fort Belvoir, VA, ETL-0248, November 1980, AD-A102619.

(2) David Lavine, Eric Olson, Barbara Lambird, Carlos Berenstein, David Leifher, Laveen Kannel; "Further Study of Digital Matching of Dissimilar Images", prepared for U.S. Army Engineer Topographic Laboratories, Fort Belvoir, VA, ETL-0385, February 1985.

(3) Robert S. Rand; "ISP Dataset Documentation"; Engineer Topographic Laboratories, Fort Belvoir, VA., 22060; In-House Report; August 10, 1984.

APPENDIX A

Control Point Information

CONTROL POINT	ISP REFERENCE	DESCRIPTION
1	410	"X" intersection of secondary and tertiary roads surrounded by (row-crop) fields; some trees.
2	430	"T" intersection of secondary and tertiary roads surrounded by fields; an almost invisible canal runs parallel to secondary road.
3	440	"T" intersection of main and tertiary roads surrounded by fields.
4	460	"X" intersection of secondary and tertiary roads surrounded by fields; an almost invisible canal runs parallel to secondary road.
5	480	"X" intersection of main and secondary roads surrounded by fields.
6	510	"T" intersection of tertiary roads surrounded by fields; an almost invisible canal runs parallel to one of the roads.
7	520	"T" intersection of secondary and tertiary roads surrounded by fields; an almost invisible canal runs parallel to tertiary road.
8	530	"T" intersection of main and tertiary road surrounded by forest on one side and fields on the other.
9	550	Bend in tertiary road with a canal running parallel; however, road and canal are obscured by adjacent forest and point appears as a corner of forest and field.
10	640	"T" intersection of main and secondary road surrounded by forest.
11	710	Overpass of main road over a highway surrounded by forest; trees obscure a canal that runs parallel to main road.
12	720	"Y" intersection of secondary and tertiary; however, trees obscure roads, and point appears as a corner of a forest and a field.

CONTROL POINT	ISP REFERENCE	DESCRIPTION
13	740	Bend in road surrounded by forest on one side and a field on the other.
14	810	"Y" intersection of a secondary road with a canal surrounded by fields; however one end of road is obscured by a line of trees.
15	820	"T" intersection of secondary and tertiary road with trees surrounded by fields.
16	830	"X" intersection of two secondary roads with trees surrounded by fields.
17	840	"X" intersection of a secondary road and an almost invisible canal with trees surrounded by fields.
18	850	"T" intersection of two secondary roads surrounded by forest on one side and fields on the other.
19	860	Boundary between a dark and light field that runs perpendicular to secondary road.
20	910	"Y" intersection of two secondary roads with a tertiary road surrounded by fields.
21	920	"X" intersection of a secondary road with a canal surrounded by fields.
22	1010	Major interchange between a highway and main road; main road passes over highway.
24	1030	Railroad passes over highway in urban area.
25	1040	"X" intersection of two secondary roads surrounded by lawns and houses in residential area.
26	1110	Secondary road passes over railroad in urban area.
27	1120	"X" intersection of main and secondary road in urban area.
28	1130	"T" intersection of main and secondary road in urban area.

CONTROL POINT	ISP REFERENCE	DESCRIPTION
29	1140	"T" intersection of highway and secondary road surrounded by fields; some trees.
30	1160	Corner of light field and dark field.
31	1210	Main road passes over railroad surrounded by trees in urban area.
32	1230	Major "X" intersection of two main roads in urban area.
33	1231	"T" intersection of major and secondary road surrounded by trees on one side and grass on the other in urban area.
34	1310	"Y" intersection of two main roads and a secondary road surrounded by some trees in urban area.
35	1330	"X" intersection of two secondary roads surrounded by buildings in urban area.
36	1340	"T" intersection of two secondary roads surrounded by buildings in urban area.
37	1350	Railroad enters a tunnel surrounded by some trees and grass in urban area.

APPENDIX B

Correlation Values for Band Combinations

CTRL PT/ WINDOW SZ		BAND COMBINATIONS								
		1&2	1&3	1&4	1&5	1&6	1&7	1&8	1&9	1&10
1	W=9	.94	.92	.89	.92	.92	.91	.15	-.61	-.44
	W=15	.91	.88	.84	.86	.86	.85	.02	-.58	-.51
2	W=9	.99	.99	.99	.99	.99	.99	.95	-.04	.17
	W=15	.99	.99	.99	.99	.99	.99	.96	-.02	.26
3	W=9	.98	.97	.95	.94	.94	.93	.27	-.79	-.79
	W=15	.97	.94	.91	.89	.87	.87	.17	-.75	-.73
4	W=9	.99	.98	.97	.96	.95	.96	.57	-.83	-.81
	W=15	.98	.97	.95	.95	.95	.94	.53	-.78	-.75
5	W=9	.98	.96	.92	.91	.91	.89	.32	-.56	-.62
	W=15	.99	.97	.93	.94	.94	.93	.45	-.36	-.44
6	W=9	.86	.79	.73	.70	.66	.65	.49	-.59	-.59
	W=15	.68	.48	.36	.26	.21	.18	.25	-.15	-.18
7	W=9	.96	.93	.89	.92	.94	.93	-.34	-.83	-.76
	W=15	.95	.91	.86	.90	.92	.90	-.44	-.83	-.79
8	W=9	.97	.96	.94	.95	.96	.94	-.09	-.64	-.64
	W=15	.97	.95	.91	.96	.96	.95	.02	-.38	-.38
9	W=9	.88	.84	.83	.84	.86	.85	.23	-.30	-.31
	W=15	.87	.84	.83	.84	.84	.84	.20	-.26	-.31
10	W=9	.99	.99	.99	.99	.99	.99	.21	-.81	-.85
	W=15	.99	.99	.99	.99	.99	.99	.23	-.82	-.84
11	W=9	.99	.99	.99	.99	.99	.99	-.17	-.88	-.71
	W=15	.99	.99	.99	.99	.99	.99	-.20	-.87	-.89
12	W=9	.54	.51	.43	.44	.42	.46	.36	.21	.27
	W=15	.73	.69	.64	.64	.65	.66	.44	.14	.21
13	W=9	.99	.95	.93	.88	.84	.82	.47	-.33	-.25
	W=15	.96	.94	.91	.90	.88	.87	.13	-.52	-.47
14	W=9	.88	.83	.80	.81	.83	.85	.47	.09	.17
	W=15	.85	.74	.67	.68	.73	.75	.22	-.04	.05

Correlation Values (continued)

CTRL PT/ WINDOW SZ		BAND COMBINATIONS 1&2	1&3	1&4	1&5	1&6	1&7	1&8	1&9	1&10
15	W=9	.93	.90	.87	.89	.89	.87	.66	.07	.31
	W=15	.90	.86	.84	.83	.81	.80	.70	.08	.46
16	W=9	.94	.92	.89	.89	.84	.80	.39	-.07	.01
	W=15	.87	.84	.80	.82	.78	.76	.37	-.12	-.04
17	W=9	.77	.78	.76	.75	.74	.73	.50	.23	.28
	W=15	.79	.77	.73	.69	.68	.68	.52	.08	.14
18	W=9	.94	.93	.91	.90	.90	.90	.30	-.12	-.11
	W=15	.93	.90	.85	.86	.82	.82	.11	-.17	-.17
19	W=9	.99	.98	.98	.96	.95	.94	.54	-.40	-.44
	W=15	.98	.97	.96	.94	.93	.92	.38	-.46	-.48
20	W=9	.98	.97	.96	.94	.92	.89	-.11	-.68	-.76
	W=15	.97	.96	.93	.91	.88	.85	-.16	-.59	-.61
21	W=9	.97	.96	.95	.95	.95	.94	.28	-.46	-.55
	W=15	.97	.95	.93	.93	.93	.92	.05	-.55	-.64
22	W=9	.98	.96	.94	.94	.94	.93	-.61	-.82	-.83
	W=15	.98	.95	.92	.94	.94	.92	-.66	-.85	-.85
23	W=9	.99	.98	.97	.97	.96	.96	-.78	-.95	-.96
	W=15	.99	.97	.94	.95	.94	.93	-.30	-.75	-.76
24	W=9	.98	.94	.87	.91	.92	.90	-.16	-.53	-.53
	W=15	.98	.95	.90	.92	.92	.90	-.13	-.60	-.60
25	W=9	.98	.95	.90	.89	.86	.82	-.18	-.50	-.58
	W=15	.98	.97	.93	.89	.85	.81	-.06	-.44	-.47
26	W=9	.98	.96	.94	.95	.95	.92	-.42	-.77	-.78
	W=15	.99	.97	.94	.92	.91	.89	-.12	-.71	-.68
27	W=9	.99	.97	.92	.91	.90	.87	-.07	-.43	-.44
	W=15	.99	.98	.96	.92	.88	.86	.33	-.16	-.19
28	W=9	.99	.98	.93	.79	.72	.67	-.06	-.58	-.56
	W=15	.99	.97	.91	.83	.80	.76	-.09	-.65	-.64

Correlation Values (continued)

CTRL PT/ WINDOW SZ		BAND COMBINATIONS								
		1&2	1&3	1&4	1&5	1&6	1&7	1&8	1&9	1&10
29	W=9	.99	.97	.94	.96	.96	.95	-.24	-.79	-.87
	W=15	.98	.95	.90	.94	.95	.94	-.41	-.79	-.80
30	W=9	.99	.98	.98	.98	.98	.98	.91	.24	.21
	W=15	.98	.95	.93	.94	.94	.94	.78	.23	.23
31	W=9	.97	.93	.93	.93	.92	.90	-.17	-.63	-.58
	W=15	.98	.97	.95	.95	.94	.93	.36	-.33	-.27
32	W=9	.97	.94	.89	.90	.90	.87	-.04	-.49	-.48
	W=15	.99	.96	.90	.92	.93	.91	-.07	-.50	-.51
33	W=9	.97	.91	.80	.82	.81	.75	-.48	-.77	-.76
	W=15	.97	.91	.77	.80	.81	.75	-.47	-.73	-.73
34	W=9	.98	.97	.96	.96	.94	.93	.23	-.36	-.39
	W=15	.98	.97	.95	.94	.93	.92	.29	-.35	-.37
35	W=9	.98	.96	.92	.88	.85	.81	.66	.45	.31
	W=15	.98	.96	.92	.88	.84	.80	.64	.36	.25
36	W=9	1.00	.99	.98	.98	.96	.89	.46	-.24	-.25
	W=15	.99	.98	.97	.97	.93	.83	.40	-.17	-.19
37	W=9	.95	.92	.90	.92	.91	.91	.07	-.28	-.25
	W=15	.94	.89	.81	.84	.84	.82	-.00	-.32	-.36

APPENDIX C. Graphs of Incremented Correlation Values

CONTROL POINT 1
Autocorrelation

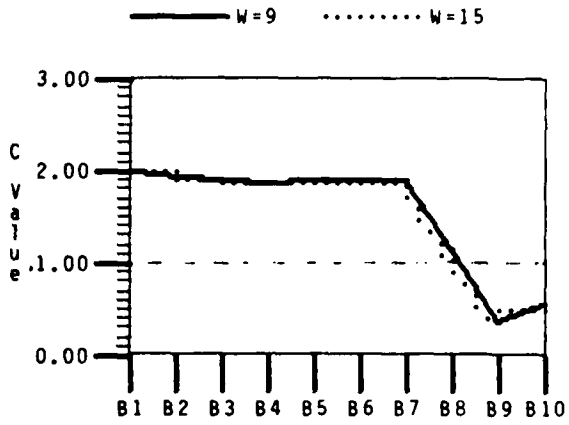

Band 1 with Band N
C Value = R + 1

CONTROL POINT 2
Autocorrelation

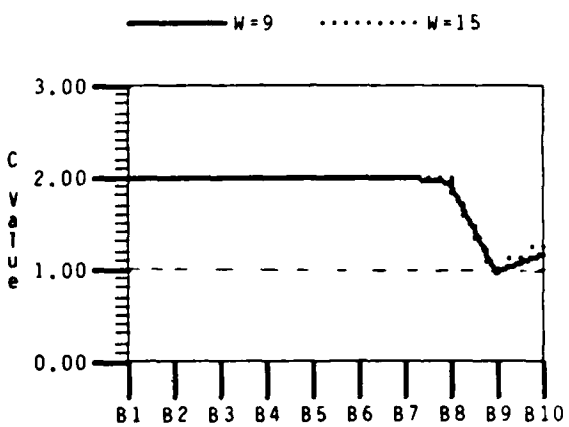

Band 1 with Band N
C Value = R + 1

CONTROL POINT 3
Autocorrelation

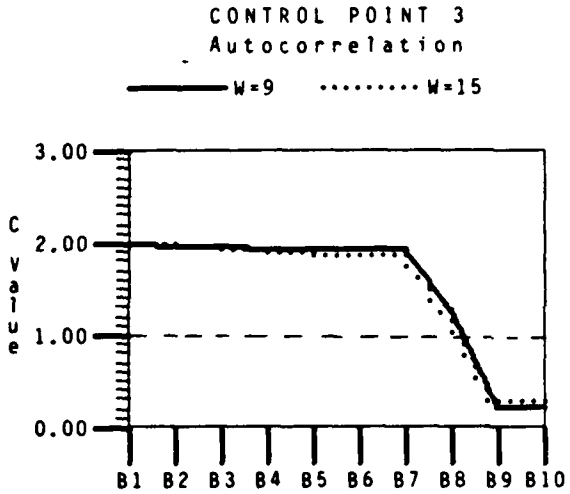

Band 1 with Band N
C Value = R + 1

CONTROL POINT 4
Autocorrelation

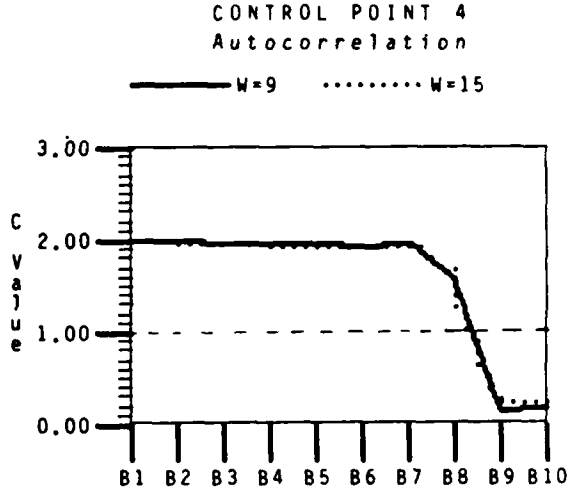

Band 1 with Band N
C Value = R + 1

CONTROL POINT 5
Autocorrelation

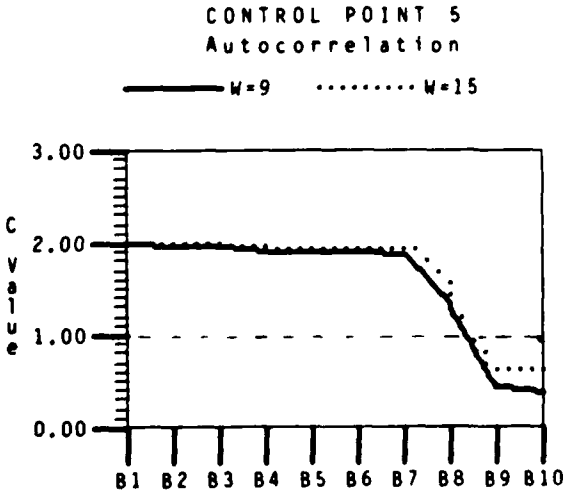

Band 1 with Band N
C Value = R + 1

CONTROL POINT 6
Autocorrelation

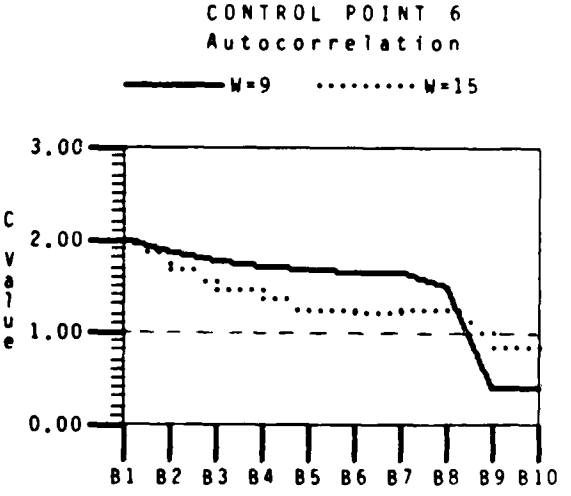

Band 1 with Band N
C Value = R + 1

CONTROL POINT 7
Autocorrelation

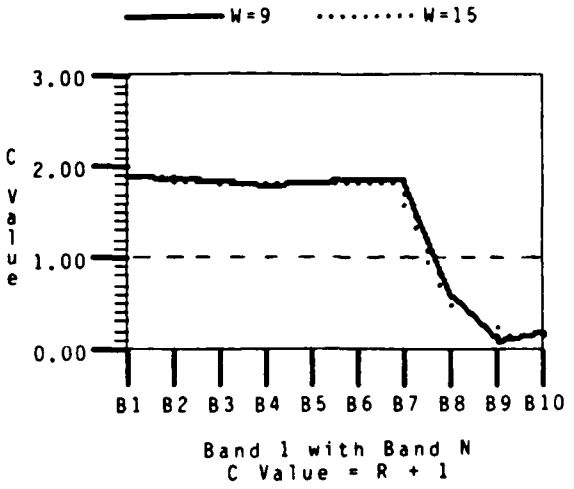

Band 1 with Band N
C Value = R + 1

CONTROL POINT 8
Autocorrelation

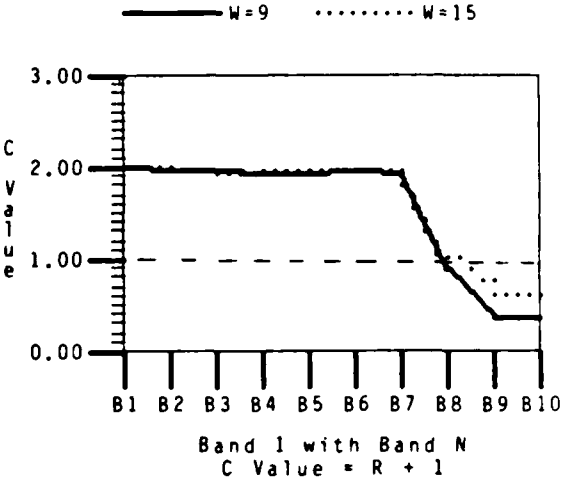

Band 1 with Band N
C Value = R + 1

CONTROL POINT 9
Autocorrelation

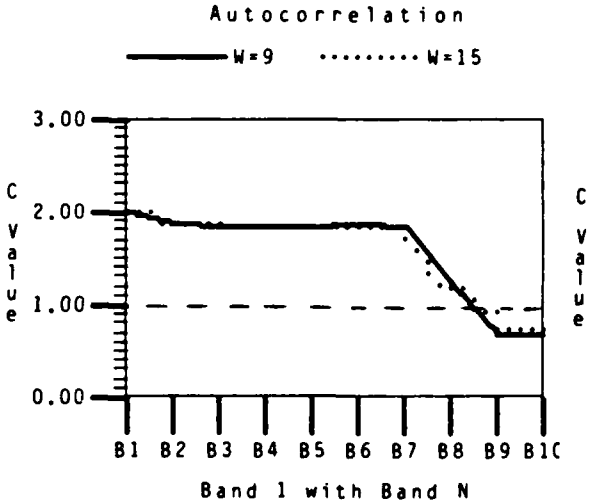

Band 1 with Band N
C Value = R + 1

CONTROL POINT 10
Autocorrelation

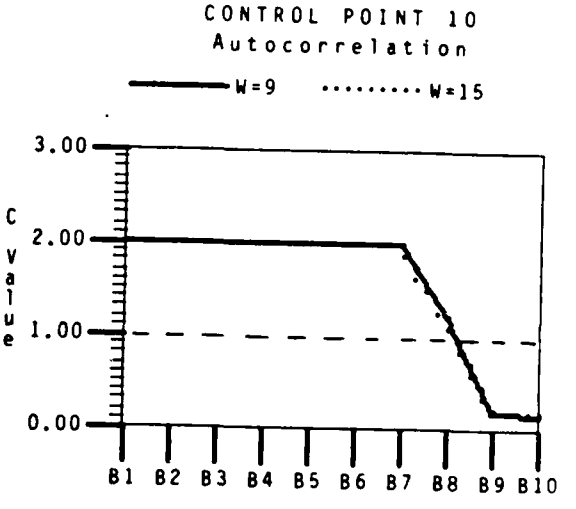

Band 1 with Band N
C Value = R + 1

CONTROL POINT 11
Autocorrelation

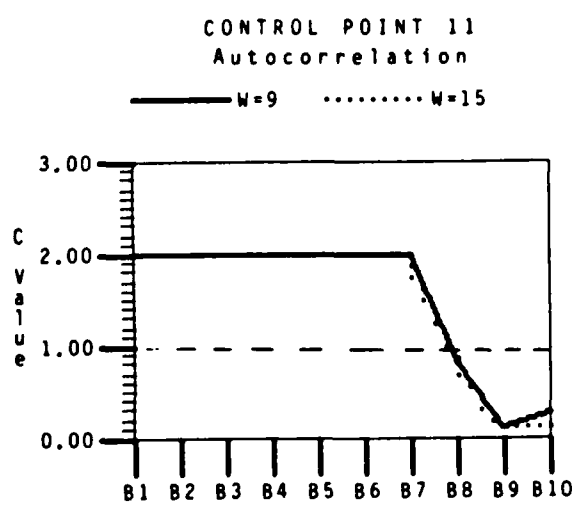

Band 1 with Band N
C Value = R + 1

CONTROL POINT 12
Autocorrelation

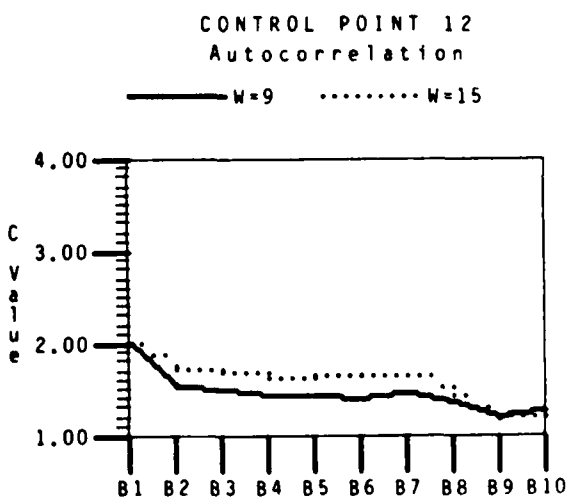

Band 1 with Band N
C Value = R + 1

CONTROL POINT 13
Autocorrelation

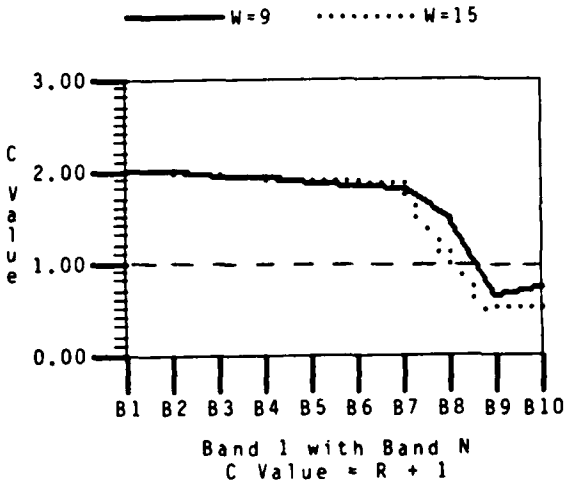

Band 1 with Band N
C Value = R + 1

CONTROL POINT 14
Autocorrelation

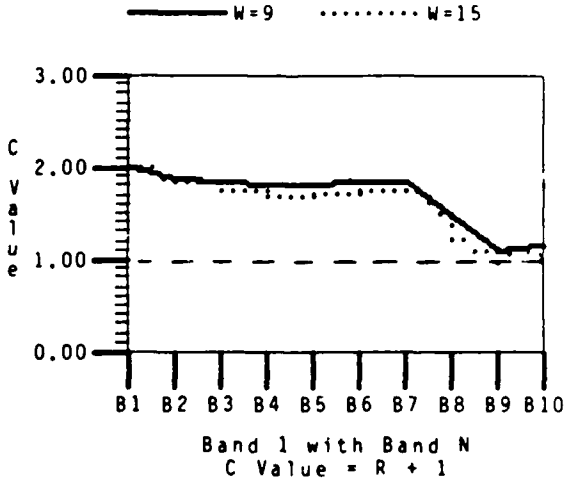

Band 1 with Band N
C Value = R + 1

CONTROL POINT 15
Autocorrelation

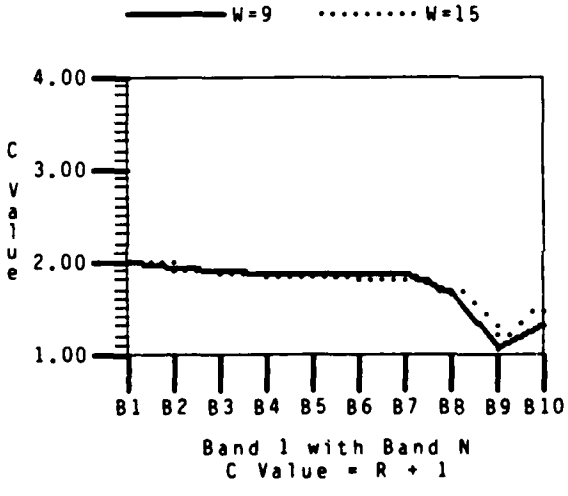

Band 1 with Band N
C Value = R + 1

CONTROL POINT 16
Autocorrelation

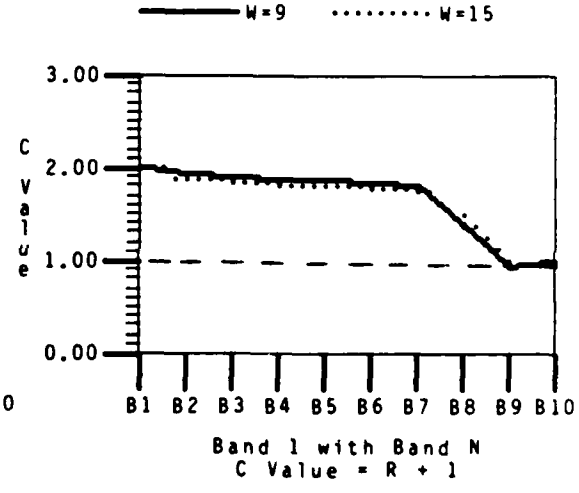

Band 1 with Band N
C Value = R + 1

CONTROL POINT 17
Autocorrelation

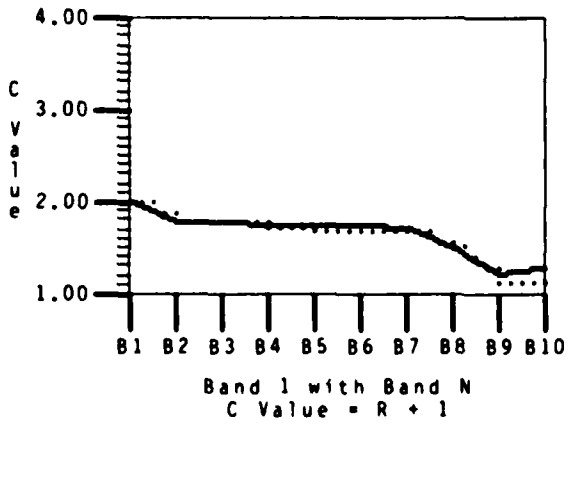

Band 1 with Band N
C Value = R + 1

CONTROL POINT 18
Autocorrelation

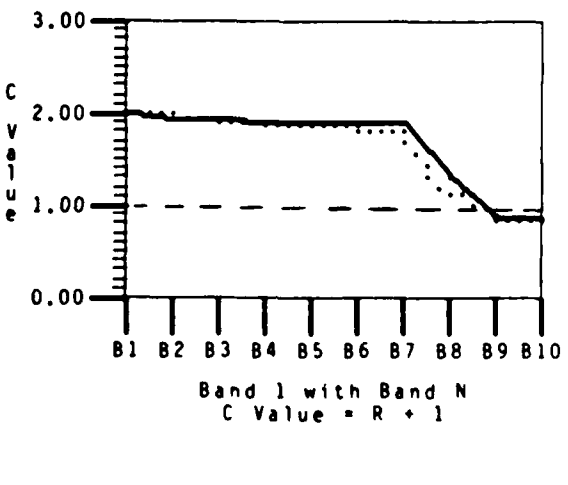

Band 1 with Band N
C Value = R + 1

CONTROL POINT 19
Autocorrelation

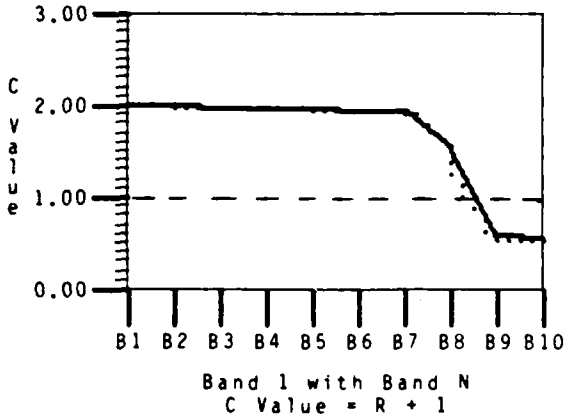

Band 1 with Band N
C Value = R + 1

CONTROL POINT 20
Autocorrelation

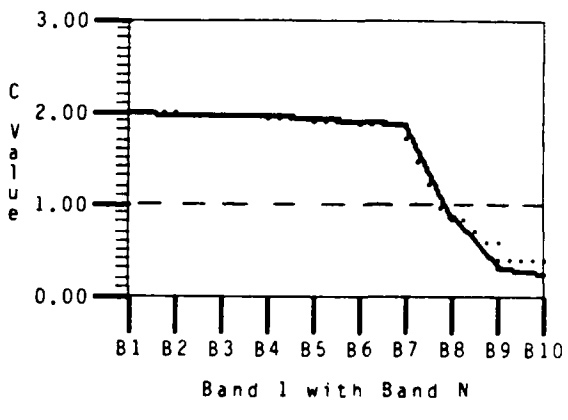

Band 1 with Band N

CONTROL POINT 21
Autocorrelation

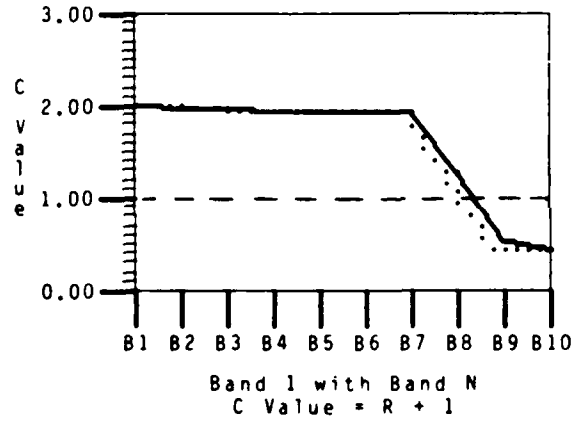

Band 1 with Band N
C Value = R + 1

CONTROL POINT 22
Autocorrelation

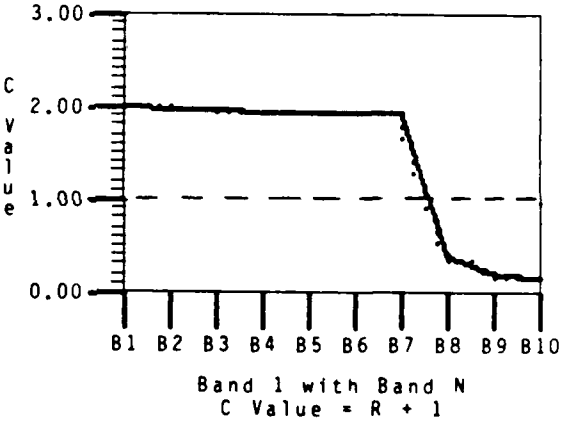

Band 1 with Band N
C Value = R + 1

CONTROL POINT 23
Autocorrelation

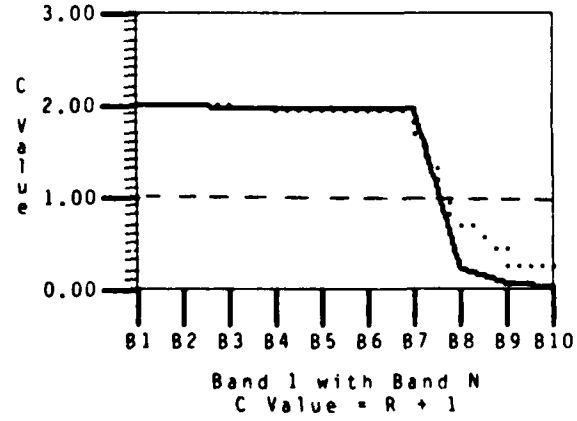

Band 1 with Band N
C Value = R + 1

CONTROL POINT 24
Autocorrelation

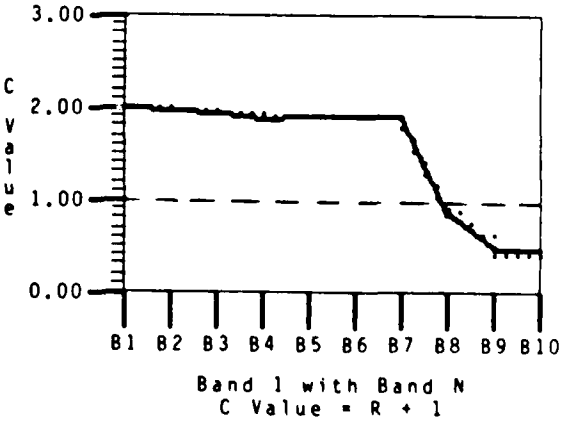

Band 1 with Band N
C Value = R + 1

CONTROL POINT 25
Autocorrelation

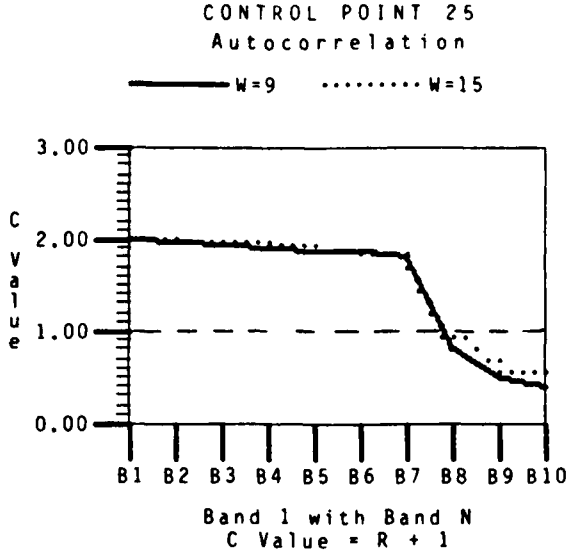

Band 1 with Band N
C Value = R + 1

CONTROL POINT 26
Autocorrelation

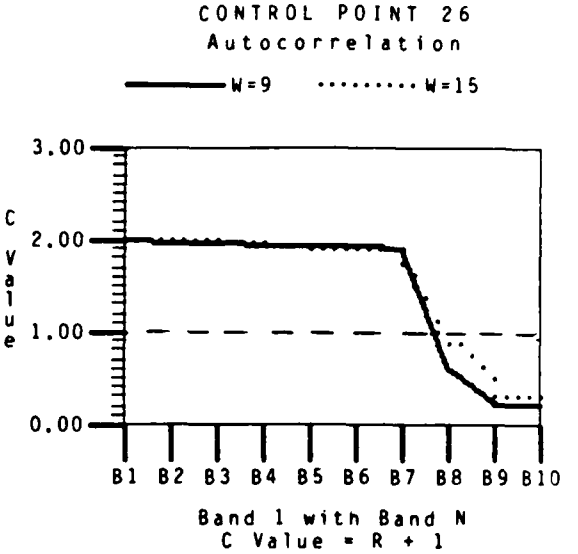

Band 1 with Band N
C Value = R + 1

CONTROL POINT 27
Autocorrelation

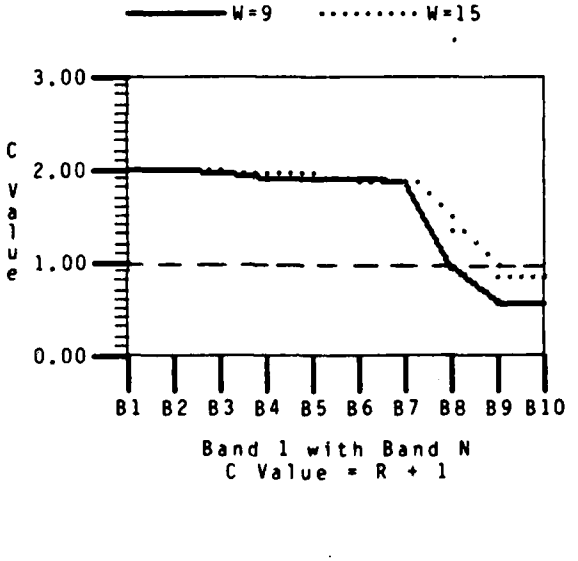

Band 1 with Band N
C Value = R + 1

CONTROL POINT 28
Autocorrelation

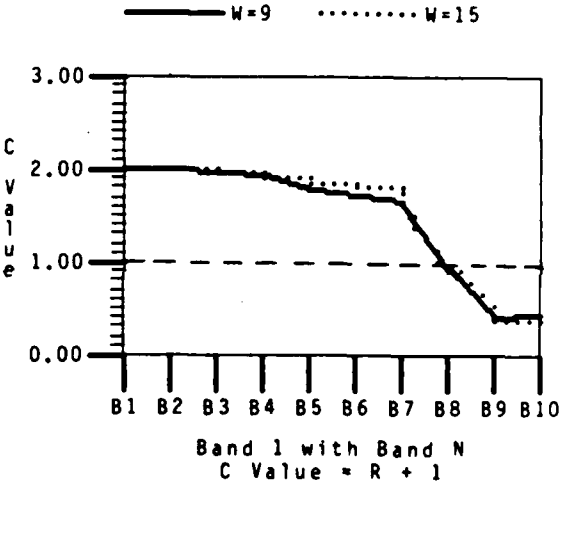

Band 1 with Band N
C Value = R + 1

CONTROL POINT 29
Autocorrelation

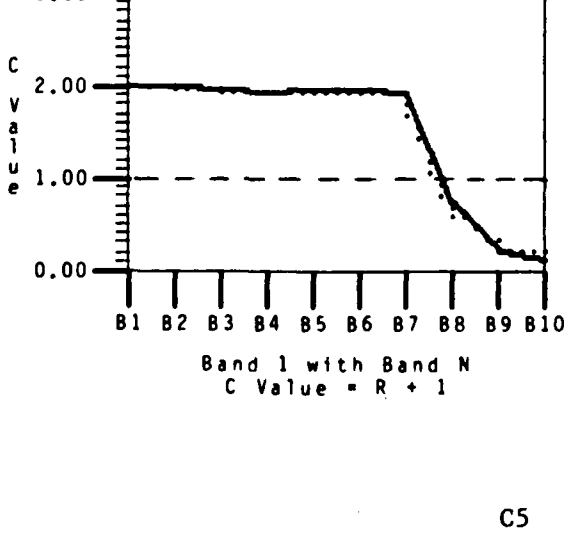

Band 1 with Band N
C Value = R + 1

CONTROL POINT 30
Autocorrelation

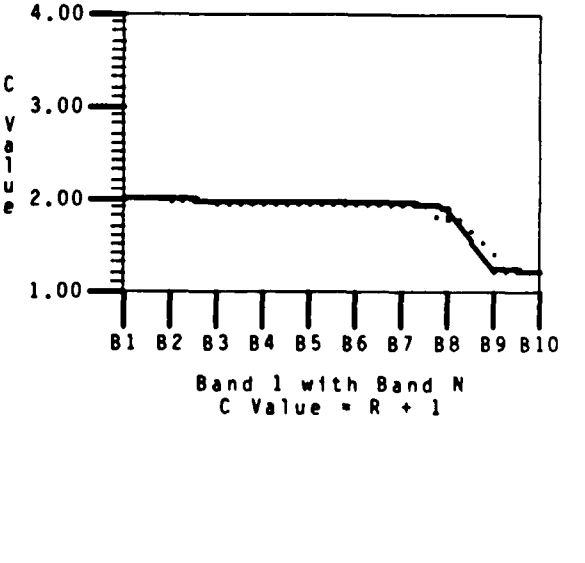

Band 1 with Band N
C Value = R + 1

CONTROL POINT 31
Autocorrelation

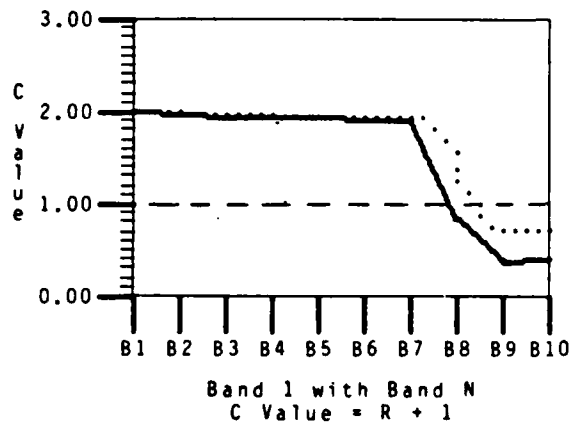

Band 1 with Band N
C Value = R + 1

CONTROL POINT 32
Autocorrelation

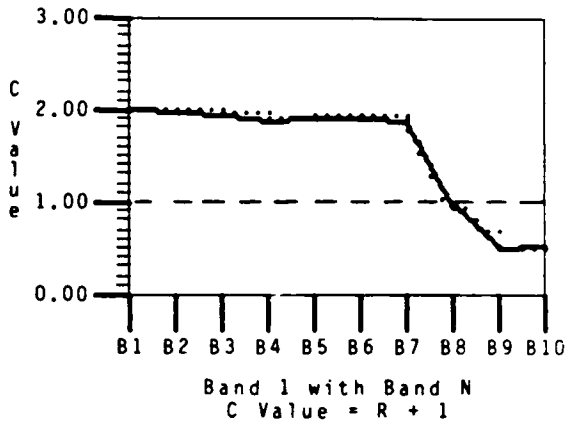

Band 1 with Band N
C Value = R + 1

CONTROL POINT 33
Autocorrelation

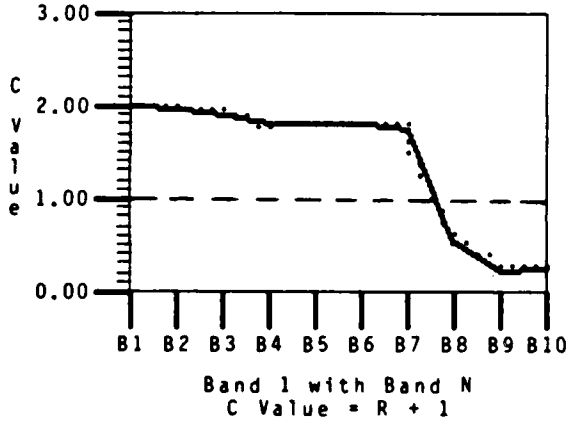

Band 1 with Band N
C Value = R + 1

CONTROL POINT 34
Autocorrelation

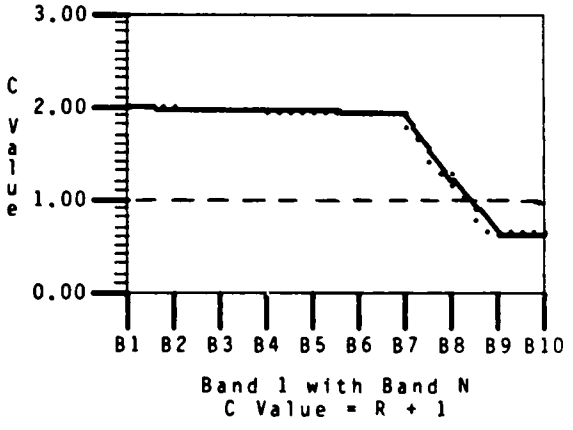

Band 1 with Band N
C Value = R + 1

CONTROL POINT 35
Autocorrelation

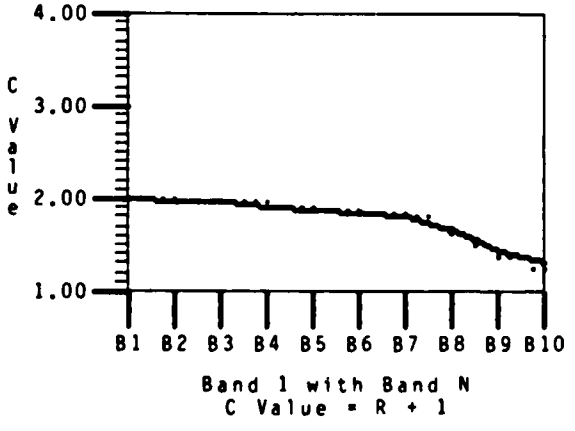

Band 1 with Band N
C Value = R + 1

CONTROL POINT 36
Autocorrelation

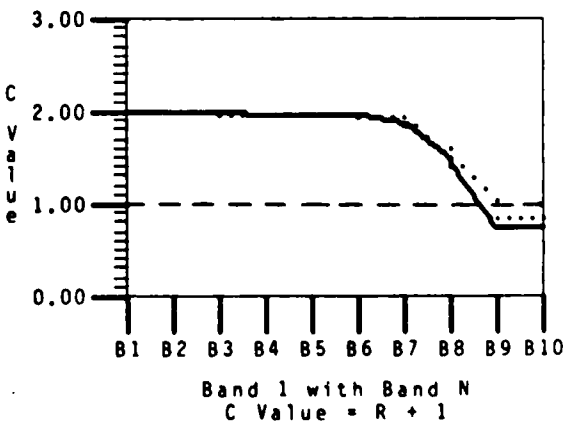

Band 1 with Band N
C Value = R + 1

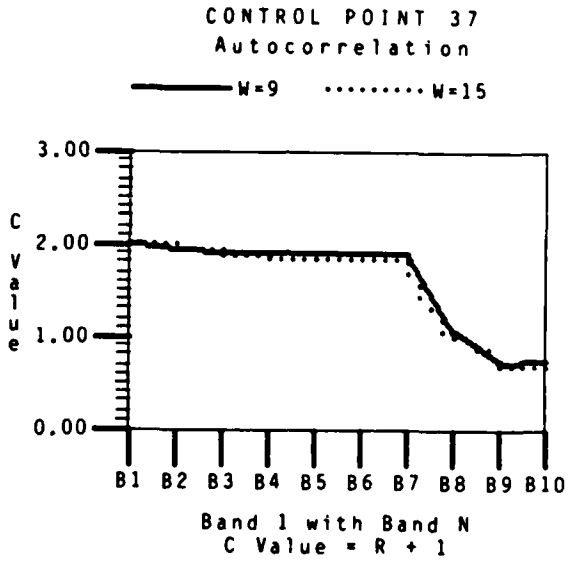
CONTROL POINT 37
Autocorrelation
W=9
W=15
3.00
2.00
1.00
0.00
C value
B1 B2 B3 B4 B5 B6 B7 B8 B9 B10
Band 1 with Band N
C Value = R + 1

APPENDIX D. Clustering of Control Points

The control points are segmented into clusters according to four thresholds of correlation, indicating the degree of difficulty that will likely be incurred in registering B1/B9 and B1/B10. The clusters reflect the data for W=9.

CLUSTER 1	CLUSTER 2	CLUSTER 3	CLUSTER 4
No Difficulty	Questionable Difficulty	Probable Difficulty	Extreme Difficulty
|R|>.79	.65<|R|<.79	.45<|R|<.65	|R|<.45
3	20	5	2
4	26	6	9
10	31	8	12
22	33	21	13
23		24	14
29		25	15
7(B9, only)	7(B10, only)	28	16
11(B9, only)	11(B10, only)	31	17
		32	18
			19
			27
			30
			34
			36
			37
		1(B9, only)	1(B10, only)
		35(B9, only)	35(B10, only)

END

FILMED

MARCH, 1988

DTIC